

Modular Analysis of Tropical Cyclones

Francis Fendell, Paritosh Mokhasi, Gregory Smetana

September 21, 2015

Nomenclature

Variables

Symbol	Description	Units
ρ	density	kg m^{-3}
p	pressure	Pa
rh	relative humidity	-
T	temperature	K
y	water vapor mass fraction	-
z	altitude	m

Constants

Symbol	Description	Value	Units
σ	ratio, molecular weights	0.622	-
c_p	specific heat capacity, const p	10^4	$\text{m}^2 \text{s}^{-2} \text{K}^{-1}$
g	gravity	9.81	m s^{-2}
L	specific latent heat, phase transition	$2.5 * 10^6$	$\text{m}^2 \text{s}^{-2}$
R	gas constant for air	287.1	$\text{m}^2 \text{s}^{-1} \text{K}^{-1}$

Subscripts

Symbol	Description
amb	ambient
eye	eye
moist	moist adiabat
s	ocean-surface value
sat	saturated
switch	lifting condensation level

trop	tropopause
underrun	underrunning moist air
v	water vapor
vsat	saturated water vapor

Contents

1	Bounding Tropical-Cyclone Intensity	2
2	Equations	4
2.1	Ambient Profiles with Altitude	4
2.2	Moist Adiabatic Profiles	4
2.3	Eye Adiabatic Profiles	5
2.4	Translation of Sea-Level Pressure Anomalies to Peak Swirl	6
3	Boundary Layer Dynamics and Energetics	6
3.1	Dynamics (unchanged from JFM work for a constant-density model)	6
3.2	Energetics	6
4	Diffusive Model of the Bulk-Vortex Module	6
5	Specifying the Position of, and Properties holding on, the Contour between the Bulk-Vortex Module and Core Module	11
5.1	Bulk-Vortex Module	12
5.2	Core Side of Contour Streamline	12
5.3	Contour Solution	13
6	Core Module: Derivation of the Streamfunction Equation (for a Tropical-Storm Scenario: no eye)	13

1 Bounding Tropical-Cyclone Intensity

Although it provides no insight into size, lifespan, precipitation, storm surge, or tornadogenesis, traditionally the one parameter taken to characterize best the intensity of a tropical cyclone is the peak sustained low-level wind speed within the vortex. Formally, NOAA takes this to be the maximal one-minute-averaged swirl speed at 10-m altitude above the air/sea interface, at any lateral distance from the center. Other meteorological agencies around the globe adopt three-minute or ten-minute averaging, and typically arrive at a lower value. (In many contexts, the tropical cyclone will continue to be characterized by the highest value achieved during its lifespan, even if the system in the meantime has declined to lower peak speed.) Also, the air/sea interface can become so convoluted and/or ill-defined under high wind shear that sometimes altitude as high as a kilometer above the nominal air/sea-interface height is adopted. In any case, although definitive values are given for the intensity of a tropical cyclone, in fact, comprehensive measurement is almost never available. In the Atlantic basin, and sometimes in the eastern North Pacific, the values often are best estimates inferred from measurements made by reconnaissance aircraft flying a few transects (legs) of the vortex at altitude of about 3 km, at intermittent intervals of time. Elsewhere in the tropics, the values for intensity are estimates from subjective interpretation of cloud imagery taken from satellites (i.e., from pattern recognition, the so-called Dvorak method). In general, any cited intensity is uncertain to within 5-10/

Accordingly, of interest is the peak swirl theoretically achievable in a given spawning ambient atmosphere, upon postulation of the physical processes occurring within the system. Here we idealize the system as a steady, axisymmetric vortex contained within a conceptual, uniformly rotating (at the angular speed of the locally normal component of the Earth's rotation), right circular cylinder with an open lateral boundary.

The cylinder has an impervious slippery isobaric isothermal horizontal lid at the altitude of the tropopause (to be defined), and an impervious no-slip nonisobaric horizontal bottom at the altitude of the nominal air-sea interface. Implicitly, there is a low-level inflow, ascent in the core near the axis of rotation (and symmetry), and upper-level outflow from the cylinder. However, we here deal minimally with the secondary (radial/axial) flow, and derive thermo-hydrostatically and cyclostrophically based bounds on the swirl speed achievable in the cylinder. We focus on sensible-heat-and-moisture content of the throughput entering the cylinder at the periphery, for a once-through transit and discharge back to the surrounding atmosphere. The intake is regarded as convectively unstably stratified, and the discharge is likely to be stably stratified.

Thus a vortex of at least tropical-depression intensity is taken to exist in the cylinder. The ambient is somewhat modified from the mean autumnal maritime-tropical sounding (e.g., Jordan ambient) because on a typical day there is no tropical cyclone present. The diffusive transfer from sea to air of heat and moisture across the bottom boundary of the cylinder is at about ambient level, and is not significantly enhanced above ambient level. The heat and moisture already present in the atmospheric intake are shown to be readily sufficient to sustain the vortex without the need for any hypothesized augmented transfer of enthalpy from the underlying ocean.

We take the adopted ambient stratification to hold at all altitudes at the periphery, even though the upper-tropospheric efflux disrupts that ambient stratification at higher altitudes in the troposphere.

Our goal is to compute the lateral pressure deficit from ambient, holding at sea level under various vertical columns of air within the vortex. For a hydrostatic approximation, the sea-level pressure is the weight per cross-sectional area of a vertical column of fluid. Thus, the sea-level pressure anomaly is an integral over altitude of the discrepancy of the local density from ambient density. If the top of the vortex is an isobaric isothermal lid, then any sea-level-pressure anomaly is owing to processes within the vortex. In particular, sea-level air rising on a moist-adiabatic locus of thermodynamic states in the idealized eyewall of a hurricane (or in the core of a well-developed tropical storm) can generate a pressure anomaly of no more than a few tens of hectoPascals (hPa, equivalent to millibars). Condensational heating, to counteract expansional cooling during ascent to lower pressure, can effect no greater density reduction. Under a cyclostrophic approximation to the conservation of radial momentum (suitable for the axisymmetric right-circular-cylinder geometry), with the radial profile of the swirl component of relative velocity being of Rankine-vortex form, and with the density being held approximately constant with radius, then the peak swirl speed cannot exceed about 40 m/s. This is the peak speed of a strong tropical storm, and substantially smaller than the speed recorded in the highest category of hurricane. To achieve the columnar reduction of density that results in a sea-level-pressure anomaly of of nearly 100 hPa or even greater, some other physical process must be involved. That process is compressional heating of relatively dry, tropopause-level air, during descent seaward to higher pressure in a central eye. The pressure deficit so achievable is far more than the magnitude that is consistent with the nearly 100 m/s peak swirl speed observed in the most intense hurricanes. In practice, the eye is not entirely dry owing to evaporative cooling related to the influx to the eye of condensate generated in the adjacent eyewall. Also, the eye may not extend the entire distance from the tropopause seaward to ocean surface; some inflowing moist air may under-run a partially inserted, central eye.

An inconsistency in the foregoing discussion is that the computation of the lateral pressure differences is at sea-level altitude. However, the swirl-speed conversion utilizes a cyclostrophic balance. A diffusion-free approximation to the conservation of radial momentum holds in the inviscid flow above the roughly one-kilometer-thickness, ocean-surface-contiguous boundary layer. Nevertheless, the adopted procedures seem a reasonable way to proceed.

The analysis that follows provides quantitative details in support of the foregoing discussion. Even so, the analysis leaves many notable details unresolved. Why do (statistically) only about half of tropical storms develop eyes, and can we anticipate which tropical storms will evolve to become hurricanes? Why do (statistically) only about one-third to one-half of hurricanes generate well-defined eyes (i.e., become major hurricanes), and can we anticipate which hurricanes will? These transitions may depend on changes in ambient conditions, but plausibly, once a tropical system achieves the levels of intensity under discussion, the transitions may depend primarily on internal thermo-fluid-dynamics. Also, the high peak swirling of a hurricane is observed near the base of the eyewall; the wind in the eye is famously calm. Hence, with increasing height, the eye/eyewall interface must slope radially outward, away from the central vertical axis, so that the density reduction in the eye may be cited plausibly as the physical mechanism supporting enhanced swirling through enhanced sea-level pressure deficit. The entrainment/detrainment between the

eye and the eyewall in a steady model remains to be explored.

2 Equations

2.1 Ambient Profiles with Altitude

(calculated from $T_{amb}[p]$, $rh_{amb}[p]$)

- Equations of State

$$p = \rho RT \quad (1)$$

$$\sigma p_v = \rho_v RT \quad (2)$$

- Definition of Water Vapor Mass Fraction

$$y = \rho_v / \rho \quad (3)$$

$$y = \sigma rh P(T) / \rho \quad (4)$$

- Definition of relative humidity

$$rh = \rho_v / P(T) \quad (5)$$

- Hydrostatics

$$\frac{\partial p}{\partial z} = -\rho g \quad (6)$$

2.2 Moist Adiabatic Profiles

Since y const, on a dry adiabat,

$$\left(\frac{T}{T_{ref}} \right)^{\frac{\gamma}{\gamma-1}} = \frac{p}{p_{ref}} = \frac{p_v}{(p_v)_{ref}} \quad (7)$$

where $\frac{\gamma}{\gamma-1} = \frac{R}{c_p}$

Let T be the lifting-condensation-level state and T_{ref} be the sea-level-ambient state

$$\left(\frac{(T_{sat})_{onset}}{(T_{amb})_\rho} \right)^{3.5} = \frac{p_v[(T_{sat})_{onset}]}{[rh]_{amb} \rho p_v[(T_{amb})_\rho]} \quad (8)$$

This gives the temperature at which surface air would saturate if lifted dry adiabatically. The temperature implies a pressure on the adiabat.

Once saturated, the moist adiabat follows the following locus of the thermodynamic states, to rough approximation (the condensate falls out):

$$c_p dT + L \sigma d\{p[T]/p\} - \frac{dp}{\rho} = 0 \quad (9)$$

where $T(P_{onset}) = (T_{sat})_{onset}$

Where this $T(p)$ curve crosses the $T_{amb}(p)$ is identified as the tropopause. The height of the tropopause is from $z_{amb}(p)$, inverse of $p_{amb}(z)$

Note: The moist-adiabat locus is based on the total energy $c_p T + Ly + gz + q^2/2 = const$, where $q^2/2$ (kinetic energy) is about a 1.5% contribution and is discarded.

Integrate from the tropopause seaward to find the thermodynamic state holding at the base $z = 0$:

$$\frac{dp}{dz} = -\rho g \quad (10)$$

$$c_p \frac{dT}{dz} + \sigma L \frac{d}{dz} [p(T)/p] - \frac{1}{\rho} \frac{d\rho}{dz} = 0 \quad (11)$$

$$p(z_{trop}) = p_{trop} \quad (12)$$

$$T(z_{trop}) = T_{trop} \quad (13)$$

Remember to drop the terms with L thenceforth if T increases in value to $(T_{sat})_{onset}$ before $z = 0$ is reached; i.e. , switch over to the dry adiabat below the lifting condensation level. Note $p_{moist}(z = 0)$

There is a self-consistency issue that may call for iteration of the moist-adiabat result. The ambient-sea-level state is adopted as the reference state for the adiabat, but is really not pertinent to a vertical column in the core. The final state computed at $z = 0$ should be used as the reference state for a second calculation of temperature vs pressure, identification of the tropopause, and assignment of altitude. Presumably, the process quickly converges, so the initial sea-level state is recovered as the sea-level state, to excellent approximation.

2.3 Eye Adiabat Profiles

Integrate seaward from the tropopause for an unsaturated eye. Thus

$$\frac{dp}{dz} = -\rho z(???) \quad (14)$$

$$c_p \frac{dT}{dz} + \sigma L \frac{d}{dz} [p(T)/p] - \frac{1}{\rho} \frac{d\rho}{dz} = 0 \quad (15)$$

$$p(z_{trop}) = p_{trop} \quad (16)$$

$$T(z_{trop}) = T_{trop} \quad (17)$$

The key new parameter here is RH , which denotes the relative humidity in the eye. If $RH = 0$, the eye is totally dry, and, for the extreme idealization, the pressure at sea level is quite decremented from $p_{amb,s}$, the sea-level ambient value (given).

We envision some evaporative cooling because condensate (ice crystals and droplets) fall into the eye and are evaporated. The value of RH could vary with altitude, but the simplest procedure is to hold it constant with height , at some value between 0 and 1. At $RH = 1$, all the heating in the eyewall owing to condensation is reversed in the eye owing to evaporation.

In the current notebook, there is an attempt to deal with a moist inflow underrunning an eye that descends only part of the distance from the tropopause to the sea surface. So for $z_{underrun} < z < z_{tropopause}$, with $z_{underrun}$ specified (if $z_{underrun} = 0$, there is no underrun), or for $p_{tropopause} < p < p_{underrun}$, with $p_{underrun}$ specified (if $p_{underrun} > (p_{moist})_{surface}$, there is no underrun), use the above equations in the eye. In the underrun, use the same equations except $RH = 1$. However, at $z = z_{underrun}$, (or $p = p_{underrun}$ - a value for one implies a value for the other), there is a contact surface: pressure p is continuous, but density ρ and temperature T are discontinuous. Also, the total energy is (dis?) continuous (within our approximation that the kinetic energy is negligible). So

$$c_p T_+ + \sigma L (RH) p(T_+)/p_{underrun} = c_p T_- + \sigma L p(T_-)/p_{underrun} \quad (18)$$

where

$$T_+ = T(z_{underrun+}, \text{known})$$

$$T_- = T(z_{underrun-}, \text{to be found})$$

$$\text{and, for completeness, if } \rho_- = \rho(z_{underrun-}),$$

$$\rho_- = p_{underrun}/(RT_-)$$

Then one integrates moist-adiabat equations

$$\frac{dp}{dz} = -\rho g \quad (19)$$

$$c_p \frac{dT}{dz} + \sigma L \frac{d[p(t)/p]}{dz} - \frac{1}{\rho} \frac{d\rho}{dz} = 0 \quad (20)$$

to $z = 0$ to find the pressure at the surface beneath a partially inserted eye.

2.4 Translation of Sea-Level Pressure Anomalies to Peak Swirl

Let swirl

$$v(r) = \begin{cases} v_{max}(r/r_{max}), & 0 < r < r_{max} \\ v_{max}(r_{max}/r), & r_{max} < r < \infty \end{cases} \quad (21)$$

This patching of a rigidly rotating core to a potential vortex (Rankine vortex) lets V_{max} be estimated from a cyclostropic balance by substitution and integration

$$\frac{v^2}{r} = \frac{1}{\rho} \frac{\partial p}{\partial r}, \quad 0 \leq r \leq \infty \quad (22)$$

provided we estimate the density ρ (e.g. ascribe ρ some average value).
For a tropical storm (no eye, so the moist adiabat holds near $r = 0$)

$$V_{max} = \left\{ \frac{2(p_{amb} - p_{moist,s})}{\rho_{amb,s} + \rho_{moist,s}} \right\}^{1/2} \quad (23)$$

For a hurricane with a partially inserted eye,

$$V_{max} = \left\{ \frac{2(p_{amb,s} - p_{eye,s})}{\rho_{amb,s} + \rho_{eye,s}} \right\}^{1/2} \quad (24)$$

For a hurricane with a fully inserted, non-rotating eye, this is no rigidly rotating core, so

$$V_{max} = \left\{ \frac{4(p_{amb,s} - p_{eye,s})}{\rho_{amb,s} + \rho_{eye,s}} \right\}^{1/2} \quad (25)$$

There is more pressure deficit for fully inserted eye, and half need not be expended maintaining a rigidly rotating core. In any case, the absence of r_{max} in the expressions for V_{max} is noteworthy (and convenient).
? , plots of total energy (ignoring kinetic energy)

$$H(z) = c_p T(z) + L \frac{\sigma(RH)p(T(z))}{p(z)} + g(z) \quad (26)$$

for the various columns is informative.

3 Boundary Layer Dynamics and Energetics

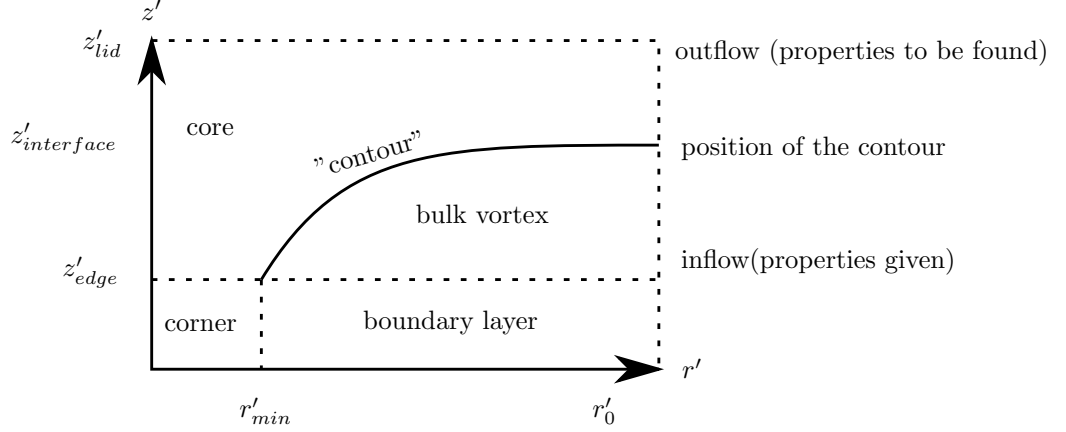
3.1 Dynamics (unchanged from JFM work for a constant-density model)

3.2 Energetics

4 Diffusive Model of the Bulk-Vortex Module

Notes:

- Prime superscript denotes a dimensional quantity



- Parameters z'_{edge} , $z'_{interface}$, r'_{min} , r'_0 given; the dimension z'_{lid} is computed in the (preliminary) tephigram method
- The efflux (mass/time) at $r' = r'_0$, $z'_{interface} < z' < z'_{lid}$ equals the influx of $r' = r'_0$, $0 < z' < z'_{lid}$. Here, known ambient conditions hold only for $r' = r'_0$, $0 < z' < z'_{interface}$, where convectively unstable stratification holds for circumstances of interest.
- In the Carrier/Hammond/George treatment, the angular momentum per unit mass, $r'v'(r', z') + \Omega'r'^2$, is constant on streamlines (inviscid treatment). Here, v' is the (relative(swirl, i.e., swirl in non-inertial coordinates rotating with the Earth at the locally pertinent angular speed Ω' , termed the Coriolis parameter. We also adopt $r'v'(r') + \Omega'r'^2 = r'_0v'_0 + \Omega'r_o'^2$, where $v'(r'_0) = v'_0$, and $0 < \varepsilon \ll 1$ where $\varepsilon \equiv v'_0/(\Omega'r'_0)$, given.
- In the CHG treatment, in the bulk-vortex modules

$$Y(r', z') = Y_{amb}(z') \equiv Y(r'_0, z') \quad (27)$$

$$E'(r', z') = E'_{amb}(z') \equiv E'(r'_0, z') \quad (28)$$

where

$$\begin{aligned} Y &\equiv \rho'_v/\rho' = \sigma(RH)P'(T')/P' \\ E &= c'_p T' + L'Y + g'z' + q'^2/2 \\ &= c'_p T + L'Y + g'z' + v^2/2 \end{aligned} \quad (29)$$

That is, the relative speed $q'^2 = u'^2 + v'^2 + w'^2 = v'^2$, and sometimes we drop even the v'^2 for tractability, as in the ambient $r' \rightarrow r'_0$. We simply cite CHG for justification for this approximation. Physically, CHG are saying that, as air entering this bulk vortex at $r' = r'_0$ moves to smaller r' , it is sinking slowly into the boundary-layer module, for compatibility with the boundary-layer solution. As the air descends to smaller z' , it takes on the properties of air that formerly occupied that position at smaller z' . We recall from the tephigram method:

$$E'_{amb}(z') \equiv c'_p T_{amb}(z') + L' Y_{amb}(z') + g' z' + \cancel{\frac{v_0^2(z')}{2}} \quad (30)$$

$$Y_{amb}(z') \equiv \sigma R H_{amb}(z') P[T'_{amb}(z')]/p'_{amb}(z') \quad (31)$$

where for a given ambient we have the data

$$T'_{amb}(p'), RH_{amb}(p') \equiv p'_v(p')/p'[T'_{amb}(p')] \quad (32)$$

Also, we have [recall that $p'(r'_0, z') \equiv p'_{amb}(z')$]

$$\frac{dp'_{amb}(z')}{dz'} = -p'_{amb}(z')g' = -[p'_{amb}(p'(z'))]g' \quad (33)$$

In other words, we need to be able to switch between the inverse functions $p'_{amb}(z') \leftrightarrow z'_{amb}(p')$. The reference state is taken to be $p'_{amb}(r'_0, 0) = p'_{ref}$, $T'_{amb}(r'_0, 0) = T'_{ref}$.

$$\sigma p'_v \equiv p'_v R' T' \quad (34)$$

$$p'(r', z') = p'(r', z') R' T'(r', z') \Rightarrow p'_{amb}(z') = \rho'_{amb}(z') R' T'_{amb}(z') \quad (35)$$

It will be convenient to approximate the equation of state for the gas as

$$p'(r', z') \approx p'_{amb}(z') T'(r', z') \quad (36)$$

in the bulk-gas module, for some purposes. This says merely that the density change in the bulk-vortex module is owing to hydrostatics mostly, because even the most intense hurricane is highly subsonic. We are also saying that we track water vapor only for its large condensational/evaporative heat; aside from that, water vapor is a trace species ($< 3\%$ by mass contribution to air).

- Since the flow is quasisteady and axisymmetric, the secondary flow is treated by the introduction of the streamfunction $\eta'(r', z')$; as the radial velocity component $u'(r', z')$ and the axial velocity component $w'(r', z')$ are given by

$$\begin{aligned} p'(r', z') u'(r', z') r' &= -\frac{\partial \eta'}{\partial z'} \\ p'(r', z') w'(r', z') r' &= \frac{\partial \eta'}{\partial r'} \end{aligned} \quad (37)$$

If the aximuthial component of vorticity, $\omega'_\theta = 0$ within the bulk-vortex module, then

$$\omega'_\theta(r', z') = -\left[\frac{\partial v'}{\partial r'} - \frac{\partial u'}{\partial z'}\right] = 0 \Rightarrow \frac{\partial}{\partial z'} \left(\frac{1}{\rho' r'} \frac{\partial \eta'}{\partial z'}\right) + \frac{\partial}{\partial r'} \left(\frac{1}{\rho' r'} \frac{\partial \eta'}{\partial r'}\right) = 0 \quad (38)$$

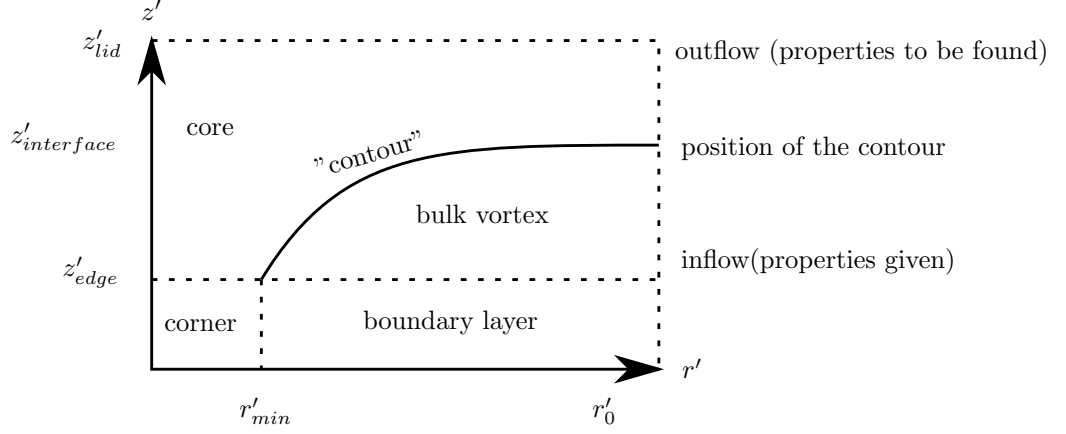
For a first cut, $p'(r', z') \rightarrow p'_{amb}(z')$ seems reasonable.

For Dirichlet boundary condition on $\eta'(r', z')$ in the bulk-vortex module,

At $r' = r'_0$:

$$\rho' u' r'_0 = -\frac{\partial \eta'}{\partial z'} \rightarrow \eta'(r'_0, z') - 0 = r'_0 \int_{z'_{edge}}^{z'} p'(r'_0, z') [-u(r'_0, z')] dz' \quad (39)$$

$$\eta'_{max} = r'_0 \int_{z'_{edge}}^{z'_{interface}} z'_{interface} p'_{amb}(z') [-u'_{in}(z')] dz' \quad (40)$$



If $[-u'_{in}(z')] = -u'_{in}$, const, then

$$\eta'_{max} = \frac{r'_0}{g'} [p'_{amb,s}(z'_{interface}) - p'_{amb,s}(z'_{edge})] (-u_{in}) \quad (41)$$

The inflow (u'_{in} follows since η'_{max} is know.

- Aside:

$$\frac{\partial p'}{\partial r'}(r'_0, z'_{edge}) \approx p'(r', z'_{edge}) \left[2\Omega' v'(r') + \frac{v'^2(r')}{r'} \right], \quad (42)$$

$p'(r'_0, z'_{edge}) = p'_{amb}(z'_{edge})$; $v'(r')$ known:

$$\begin{aligned} r' v'(r') + \Omega' r'^2 &= r'_0 v'(r'_0) + \Omega' r_0'^2 \\ \rho'(r', z'_{edge}) &= p'(r', z'_{edge}) / [R' T'(r', z'_{edge})] \\ c'_p T'(r', z'_{edge}) + L' Y(z'_{edge}) + g' z'_{edge} + \frac{v'^2(r')}{2} &= E'_{amb}(z'_{edge}) \end{aligned} \quad (43)$$

This yields a good approximation to $p'(r'_{min}, z'_{edge})$

- Returning to estimation of $\eta'_{max} = \eta'(r'_{min}, z'_{edge})$:

$$\eta'(r', z_{edge}) - 0 = \int_{r'_0}^{r'} \underline{r}' p'(\underline{r}', z'_{edge}) w'(\underline{r}', z'_{edge}) d\underline{r}' \quad (44)$$

From boundary-layer dynamics,

$$\eta'_{max} = \int_{r'_{min}}^{r'_0} \underline{r}' p'(\underline{r}', z'_{edge}) [-w'_{BLedge}(\underline{r}')] d\underline{r}' \quad (45)$$

The entrainment into the boundary layer is estimated on an incompressible basis (constant-density treatment of the dynamics), but we accept this approximation. The density $\rho'(r', z'_{edge})$ is discussed just above. The quantity η'_{max} is an enormous number in SI units, and we use it for normalization of $\eta(r', z')$ for computational convenience! So we deal with

$$\eta(r, z) = \eta'(r', z')/\eta'_{max} \quad (46)$$

where $r = r'/r'_0$, $z = z'/z'_{lid}$. We cannot readily non-dimensionalize z' against r'_0 because $r'_0 \gg z'_{lid}$. It is true that r'_{min} is closer to z'_{lid} in size, but I prefer not to use it for non-dimensionalization. We could use $[\nu'/(2\Omega')]^{1/2}$ for non-dimensionalizing z' in the bulk-vortex module, since $z'_{interface} \approx 3(z'_{edge})$ and $z'_{edge} \sim 5 \left(\frac{\nu'}{2\Omega'} \right)^{1/2}$. I did not want to do this when the bulk-vortex module was being treated as inviscid, but now only the dynamics (not the energetics) is inviscid in the bulk-vortex module.

- The pressure field in the bulk-vortex module is given by inviscid dynamics:

$$\begin{aligned} \frac{\partial p'}{\partial z'} &= -\rho g' \\ \frac{\partial p'}{\partial r'} &= p' \left[2\Omega' v' + \frac{v'^2}{r'} \right] \\ p'(r'_0, z') &= p'_{amb}(z') \\ p'(r'_0, 0) &= p'_{ref} \end{aligned} \quad (47)$$

Conveniently,

$$p'(r', z') - p'(r'_0, z'_{edge}) \doteq -g' \int_{z'_{edge}}^{z'} p'_{amb}(z') dz' - \int_{r'}^{r'_0} p'(\underline{r}', z'_{edge}) \left[2\Omega' v'(\underline{r}') + \frac{v'^2(\underline{r}')}{\underline{r}'} \right] d\underline{r}' \quad (48)$$

This approximation gives the pressure field to better accuracy along the top edge of the boundary and at the periphery, but less accurately elsewhere. Thus, the contour is given relatively accurately near its end "points" (r'_{min}, z'_{edge}) and $(r'_0, z'_{interface})$.

In the above expression for $p'(r', z')$, $p'(r'_0, z'_{edge}) = p'_{ref}$. Also, integration yields $p'(r', z'_{edge})$. (See page ?), and $T'(r', z'_{edge})$ is available from the expression $E'(r', z'_{edge}) = E'_{amb}(z_{edge})$ (see page ?). Thus $\rho'(r', z'_{edge}) = p'(r', z'_{edge})/[R'T'(r', z'_{edge})]$.

- Also,

$$\frac{\rho'(r', z')}{c'_p} = \ln \left\{ \frac{[T'(r', z')/T'_{ref}]}{[p(r', z')/p'_{ref}]^{\frac{\gamma-1}{\gamma}}} \right\} \quad (49)$$

or

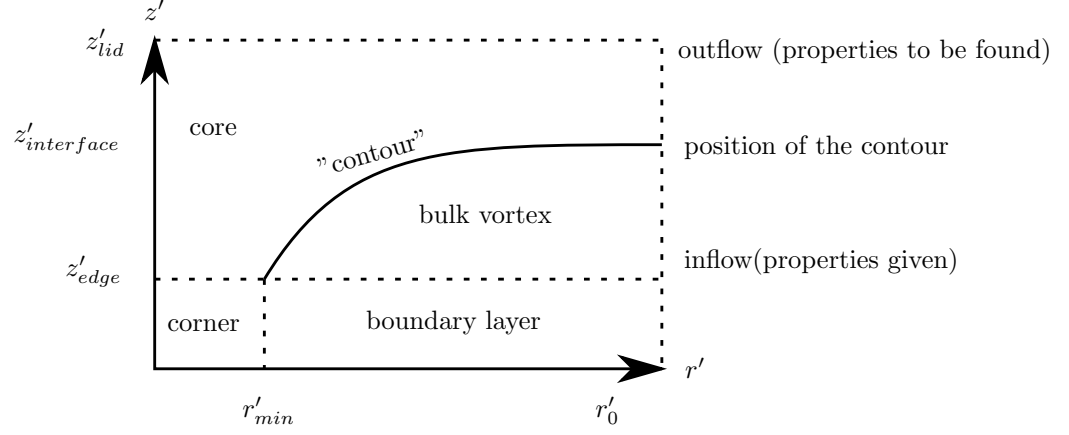
$$\frac{s'(r', z')}{R'} = \ln \left\{ \frac{[T'(r', z')/T'_{ref}]^{\frac{\gamma}{\gamma-1}}}{[p(r', z')/p'_{ref}]} \right\} \quad (50)$$

- To within $2\frac{1}{3}\%$, with $L' = 2.5 * 10^6 \text{ J kg}^{-1} \dots$

I give more accurate expressions in the notebook. Nominally, freezing is at 273K, but in fact in the atmosphere, freezing occurs closer to 263 or 253K.

- Notice that a reconnaissance flight at 10kft flies in the core module.

5 Specifying the Position of, and Properties holding on, the Contour between the Bulk-Vortex Module and Core Module



- We seek to define the curve ("contour") between (r'_{min}, z'_{edge}) and $(r'_0, z'_{interface})$, given end points.
- The contour position is defined by continuity of pressure $p'(r', z')$ because the dynamics on each side is inviscid. The swirl $v'(r', z')$ is continuous across the contour, but the radial velocity component $u'(r', z')$ and axial velocity component $w'(r', z')$ are discontinuous, so the contour is a vortex sheet for the "secondary flow." The pressures $p'(r'_{min}, z'_{edge})$ and $p'(r'_0, z'_{interface})$ are known from the bulk-vortex analysis, with $p'(r'_{min}, z'_{edge}) > p'(r'_0, z'_{interface})$ in cases of interest.
- The temperature and density are discontinuous across the contour, which is a contact surface. The air is unsaturated in the bulk-vortex module, and saturated in the core module.
- The contour is a streamline: there is no flow across it.
- The entropy, angular momentum, and total stagnation energy are constant on streamlines on the core side, which is inviscid. The value of each variable varies from streamline to streamline
- Only the angular momentum is constant on streamlines on the bulk-vortex side, and for tractability, we examine only the special case for which the constant is invariant from streamline to streamline. Thus the model for the swirl in the bulk-vortex model is a potential vortex, generalized to the non-inertial coordinate system.
- We anticipate that the pressure $p'(r', z')$ on the contour decreases monotonically from $p'(r'_{min}, z'_{edge})$ to $p'(r'_0, z'_{interface})$, and that the curve $z'_{contour}(r')$ has monotonically decreasing but non-negative slope as one goes from (r'_{min}, z'_{edge}) to $(r'_0, z'_{interface})$. (The inverse representation $R'_{contour}(z')$ has a monotonically increasing and non-negative slope.) According to our model, r'_{min} decreases, but z'_{edge} , r'_0 , and $z'_{interface}$ do not change, as the vortex intensifies, so the contour shape is not anticipated to be a sensitive indicator of intensity for a fixed ambient. The position r'_{min} is a sensitive indicator of intensity.

5.1 Bulk-Vortex Module

- Conservation of angular momentum

$$r'v'(r') + \Omega'r'^2 = r'_0v'_0 + \Omega'r_0'^2 = \Omega'r_0'^2(1 + \varepsilon) = \Gamma'_0 \quad (51)$$

- Pressure field

$$p'(r', z') - p'(r'_0, z'_{edge}) \doteq g' \int_{z'_{edge}}^{z'} \rho'_{amb}(z') dz' - \int_{r'}^{r'_0} \rho'(\underline{r}', z'_{edge}) \left\{ 2\Omega v'(\underline{r}') + \frac{v'^2(\underline{r}')}{\underline{r}'} \right\} d\underline{r}' \quad (52)$$

The two integrals can be tabulated ahead of time. Recall that $\rho'(r', z'_{edge})$ is obtained in the bulk-vortex module equations. We much prefer this algebraic approximation for $p'(r', z')$ than to deal with a differential-equation/algebraic-equation mixture in defining the contour.

5.2 Core Side of Contour Streamline

$$r'v'(r') + \Omega'r'^2 = \Gamma'_0 \quad (53)$$

- 4 eqs for 4 unknowns: $T'_{core}(r'_{min}, z'_{edge})$, $T'_{core}(r'_0, z'_{interface})$, E'_{core} , S'_{core}

$$E'_{core}(r'_{min}, z'_{edge}) \doteq c'_p T'_{core}(r'_{min}, z'_{edge}) + \frac{L'\sigma p'[T'_{core}(r'_{min}, z'_{edge})]}{p'(r'_{min}, z'_{edge})} + g'z'_{edge} + \frac{v'^2(r'_{min})}{2} \quad (54)$$

$$E'_{core}(r'_{min}, z'_{edge}) = E'_{core}(r'_0, z'_{interface}) = c'_p T'_{core}(r'_0, z'_{interface}) + \frac{L'\sigma p'[T'_{core}(r'_0, z'_{interface})]}{p'(r'_0, z'_{interface})} + g'z'_{interface} + \frac{v'^2(r'_0)}{2} \quad (55)$$

$$\frac{S'_{core}(r'_{min}, z'_{edge})}{R'} = \ln \left(\frac{T'_{core}(r'_{min}, z'_{edge})}{T'_{ref}} \right)^{\frac{\gamma}{\gamma-1}} - \ln \left(\frac{p'(r'_{min}, z'_{edge})}{P'_{ref}} \right) + \frac{L'\sigma p'[T'_{core}(r'_{min}, z'_{edge})]}{R'T'_{core}(r'_{min}, z'_{edge})p'(r'_{min}, z'_{edge})} \quad (56)$$

$$T'_{ref} = T'(r'_0, 0), \quad p'_{ref} = p'(r'_0, 0) \quad (57)$$

$$\frac{S'_{core}(r'_{in}, z'_{edge})}{R'} = \frac{S'_{core}(r'_0, z'_{interface})}{R'} = \ln \left(\frac{T'_{core}(r'_{min}, z'_{edge})}{T'_{ref}} \right)^{\frac{\gamma}{\gamma-1}} - \ln \frac{p'(r'_{min}, z'_{edge})}{p'_{ref}} + \frac{L'\sigma p'[T'_{core}(r'_0, z'_{interface})]}{R'T'_{core}(r'_0, z'_{interface})p'(r'_0, z'_{interface})} \quad (58)$$

- Pressure field

$$E'_{core}(r'_{min}, z'_{edge}) = c'_p T'_{core}(r', z') + \frac{L'\sigma p'[T'_{core}(r', z')]}{p'(r', z')} + g'z' + \frac{v'^2(r')}{2} \quad (59)$$

$$\frac{p'(r', z')}{p'_{ref}} = \left(\frac{T'_{core}(r', z')}{T'_{ref}} \right)^{\frac{\gamma}{\gamma-1}} - \exp \left[-\frac{S'_{core}(r'_{core}, z'_{edge})}{R'} + \frac{L'\sigma p'[T'_{core}(r', z')]}{R'T'_{core}(r', z')p'(r', z')} \right] \quad (60)$$

5.3 Contour Solution

- The three equations (*) are three coupled non-linear algebraic equations for $[r', z', T'_{core}(r', z')]$ where r', z' is the point on the contour where the pressure is $p'(r', z')$, an assigned value within the range $p'(r'_{min}, z'_{edge}), p'(r'_0, z'_{interface})$
- This is a step-by-step progression, starting from one end point on the contour, and proceeding to the other end point on the contour. The first guess at the next point in the progression is the triplet of results holding at the last converged point.
- This is a parametric solution:

$$r'[p'], \quad z'[p'], \quad T'_{core}[p'] \quad (61)$$

Of course, one of the other variables could have been selected as the parameter, at least in theory.

- In the bulk-vortex module

$$\frac{S'(r', z')}{R'} = \ln \left(\frac{T'(r', z')}{T'_{ref}} \right)^{\frac{\gamma}{\gamma-1}} - \ln \left(\frac{p'(r', z')}{p'_{ref}} \right) \quad (62)$$

The core-side streamline at the contour spends so little time in the boundary layer no angular momentum is lost, but the onset of saturation changes density, temperature, vapor mass fraction, and entropy across the contour.

6 Core Module: Derivation of the Streamfunction Equation (for a Tropical-Storm Scenario: no eye)

- The core model is steady, axisymmetric, inviscid, and saturated.
- so the vapor mass fraction $Y' \rightarrow Y'_\rho(T', p')$, where $p'(T')$ given,

$$Y'_\rho(T', p') = \sigma \frac{p'(T')}{p'} = 0.622 \frac{p'(T')}{p'} \quad (63)$$

Note: Sometimes I write $p'(T')$ as $p'_\rho(T')$, an old habit. Y' is a contradiction because prime denotes dimensional, and the vapor mass fraction is dimensionless, but I reserve the symbol y for a normalized vapor mass fraction.

- y' is not conserved on streamlines $\eta'(r', z')$ owing to condensation.
- So there are just three integrals that are constant on streamlines in the core:

$$E'(\eta') = c'_p T' + L' Y'_\rho(T', p') + g' z' + q'^2/2 \quad (64)$$

where we often approximate $q'^2/2 \rightarrow v'^2/2$ but more generally $q'^2 = u'^2 + v'^2 + w'^2$

$$S'(\eta') = c_p \ln(T'/T'_r) - R'_a \ln(p'/p'_r) + L' Y'_\rho(T', p')/T' \quad (65)$$

where

$$T'_r \equiv T'_{ref} \equiv T'(r'_0, 0) = T'_{amb}(0) \quad (66)$$

$$P'_r \equiv p'_{ref} \equiv p'(r'_0, 0) = p'_{amb}(0)$$

$$\Gamma'(\eta') = r' v' + \Omega' r'^2 \quad (67)$$

- $p'/p'_r = (p'/p'_r)(T'/T'_r)$
- Solving the S' equation for p'/p'_r , and substituting for $L' Y'_\rho$ from the E' equation gives